Agronomy Research **16**(4), 1569–1579, 2018
https://doi.org/10.15159/AR.18.166

Assessment of *Calotropis* natural dye extracts on the efficiency of dye-sensitized solar cells

A.H. Alami[1,2,*], K. Aokal[2], D. Zhang[1,2], M. Tawalbeh[1], A. Alhammadi[1] and A. Taieb[1]

[1]University of Sharjah, Sustainable and Renewable Energy Engineering Department, AE2727272 Sharjah, United Arab Emirates
[2]University of Sharjah, Centre for Advanced Materials Research, AE27272 Sharjah, United Arab Emirates
[*]Correspondence: aalalami@sharjah.ac.ae

Abstract. This work presents the construction and testing of solar cells sensitized with natural dyes extracted from plants indigenous to the desert. *Calotropis* plants are self-sufficient as they grow in very harsh environments, and yet are not consumed by humans or livestock due to their irritating agents to the skin and eyes. The energy generators of these plants are the leaves, which are crushed and processed to produce the dye solution. Also, the *Calotropis* leaves are covered in a white powder that is thought to aid in mitigating the heat by scattering incident radiation. This powder material is examined and added to the dye as it proved advantageous for the overall cell efficiency, which reached 0.214% compared with 0.108% for cells with no powder. The produced cells are also compared with ones sensitized by spinach, another common natural sensitizer for dye-sensitized solar cells, and the performance proved to be significantly better. The fact that *Calotropis* is a non-food plant is an added advantage to utilizing it as a dye source, along with its intrinsic heat resistance that allows it to survive the harsh desert conditions all year round.

Key words: *Calotropis*, dye-sensitized solar cells, natural dyes.

INTRODUCTION

Photovoltaic (PV) solar energy systems are growing rapidly worldwide with an average annual rate of 6.8% and about 50 GW of new instillations every year (BNEF, 2015; Breyer et al., 2017). It is also estimated that this growth will continue and would reach around 206 GW in 2040 (REN21, 2016) and the speculated cumulative PV instillations by 2050 would be around 4,512 GW (Smith & Bogust, 2018). In specific, it is speculated by the United States Department of Energy that the electricity production through solar energy systems may count for 27% of the total electricity produced in the U.S by 2050 (Liu et al., 2018).

Geographic location and climatological conditions play a vital role in determining the performance and efficiency of any PV system (Makrides et al., 2010). Solar irradiance and temperature are the most important meteorological parameters that influence the performance of PV systems (Wang et al., 2017). Hence, the PV system's power output fluctuates throughout the day and from season to season based on the

variation of the temperature and irradiance spectrum (Kaltiya et al., 2014; Phinikarides et al., 2015).

The United Arab Emirates (UAE), lies between 22°30′ and 26°10′ north latitude and between 51° and 56°25′ east longitude which provides a basis of good solar energy exposure. This high solar exposure suggests that PV technology has a great potential as alternative power source in the future of UAE. Combining that with the region's sub-tropical and arid climate, it has been regarded as a potential to establish several PV power plants (Said et al., 2018).

Nowadays, there are three main generations of solar cell technologies. The first generation is the most commonly used. It includes monocrystalline and polycrystalline silicon cells produced from wafers that differ by crystallization levels, where each wafer can supply 2–3 watt power. The highest recorded lab efficiency achieved for this technology was around 25% (Wu et al., 2015; Polman et al., 2016). However, silicon solar cells are rigid, they have a harmful impact on the environment, their production requires a considerable amount of energy, and therefore a high production cost (Sherwani et al., 2010; Wu et al., 2015). The second generation solar cells are usually termed thin films due to their relatively thin semiconducting layer, which can be up to a few micrometres thick. This technology is based on amorphous silicon, copper indium gallium diselenide (CIGS) and cadmium telluride (CdTe). The cost of the second generation solar cells is relatively low, though, their efficiency is lower when compared to the first generation with a lab efficiency close to 18.4% (Hosenuzzaman et al., 2015; Ghosh, 2017). However, gabs frequently generated especially when manufacturing large cells due to the lack of uniformity. This leads to module efficiencies lower than the lab efficiency mentioned earlier. For instance, the best module efficiency for copper indium gallium diselenide (CIGS) and cadmium telluride (CdTe) are 13.4% and 10.7%, respectively (Sharma et al., 2017).

Third generation solar cells are the ones that use non-silicon based components and they categorized to four main types: nano crystal based, polymer based, concentrated, and dye-sensitized solar cells (Choubey et al., 2012). Third generation solar cells are not restrained by the Shockley Quieisser limit (Shockley & Queisser, 1961) and they offer the possibility of facile large-scale production with reliance on materials that are readily available and potentially inexpensive. Nevertheless, their performance and stability are restricted when compared to first and second generation technologies. This has prompted extensive studies in the technology. The efficiency for the third generation varies depending on the base of the solar cell. For instance, the dye sensitized solar cell efficiency is around 10% while the organic and nanotech solar cell is about 3–8% (Sharma et al., 2015).

Dye-sensitized solar cells are one of the most common third generation technologies with their active materials solely comprised of the dye material and an electrolyte. DSSCs are photonic devices that convert light into electricity. Their structures comprise of a porous semiconducting thin film with adsorbed dye molecules. Inspired by photosynthesis- the natural process that plants use to convert sunlight into energy, they have received considerable attention since O'Regan and Gratzel reported an -initially- outstanding high conversion efficiency of nearly 10% (O'Regan & Gratzel, 1991) using nanocrystalline mesoporous TiO_2 films. These films can be prepared using simple techniques such as: spin coating, dip coating, and screen printing.

Since UAE is a desert area, it experiences extremely hot temperatures most of the year. Despite that this harsh climate, there are more than 678 types of terrestrial plant species acclimatized to this climate. The main types of these terrestrial are ferns, flowering plants, ryophytes and mosses (Raghwa et al., 2014). One of the abundant plants in UAE is the *Calotropis* and it is the subject of this study. *Calotropis*, also known as Sodom's apple milkweed, is one of the most popular and spread flowering plant in UAE, which can easily grow in very poor soils. It belongs to Apocynaceae family, about 2.5–6 meter-tall and has white and purple waxy flowers grouped as clusters (Rahimi, 2015). Plants develop normally adaption mechanisms to survive the light fluctuations in its environment. They may adapt either by controlling the light absorption capacity or by controlling the amount of light energy being captured (Jones & Rotenberg, 2011). They optimize light absorption by adjusting the leaf orientation aiding the plants to cope with the excess amount of solar radiation especially at midday. Under extreme lighting conditions, the plants accumulate excess excitation energy that will inevitably lead to photoinhibition and further reduction in the photosynthetic efficiency. Desert plants, in particular, enter a stage where they go into energy storage mode, and all energy harvested from solar radiation goes into providing sustenance to the embryos. These embryos will dry up at a certain point and be transported in air to plant themselves away from the mother plant. Another mechanism with which plants resist excess solar absorption is by changing the deep green colour of the leaves into a pale shade of yellow that absorbs light mostly in the UV region, instead of the former case of mid-visible wavelengths.

Due to the natural origins, it is well known and expected that the extracted natural dyes contain more than one pigments. The mixed composition of the natural dyes generally does not hinder the operation of DSSCs; on the contrary, the blended dyes usually exhibit extended absorption range well beyond that of a single pigment which is beneficial for improving cell efficiency (Chang & Lo, 2010).

Spinach is a well-studied chlorophyll-based natural sensitizer containing mostly chlorophyll-a and chlorophyll-b [Journal of Alloys and Compounds 495 (2010) 606–610]. By comparing the UV-Vis absorption spectrum of dye solutions extracted from Calotropis against spinach (as shown below), it can be observed that similar to spinach, the natural dyes from Calotropis contains mostly chlorophyll-a and chlorophyll-b, as indicated by the absorbance peaks at ~ 470 nm and ~ 660 nm. As future work, the detailed composition and purity of the pigments may be determined by spectro-photometry of chlorophylls to which separate chlorophyll content could be assessed in accordance to the absorbance of the pigment extract at its characteristic wavelength. The equations, first populated by Arnon, follow a certain trend for extraction and aim to provide absorbance coefficients for resolving the two chlorophylls in the mixture depending on the chosen solvent (Ritchie, 2006).

This work investigates using a natural sensitizer extracted from Calotropis, a plant indigenous to the deserts of Sharjah, United Arab Emirates, for natural dye-sensitized solar cell applications. The plant in question is a non-food item, as compared with other natural green sensitizers such as spinach. The latter will be used to sensitize another set of cells for benchmarking purposes, as it is one of the popular natural sensitizers. Since the leaves of the plant also feature a powder material on its surfaces, the effect of adding this powder to the sensitizing dye will also be examined. A detailed account on cell components selection and construction will be given, as well as an electrochemical cell impedance analysis, and cell performance parameters. The proposed dye material comes

from a plant that is abundant, adaptive to harsh environmental conditions and also inconsumable as source of sustenance for people and livestock makes it a very attractive natural sensitizer both ecologically and economically. This being said, the obtained results are not expected to surpass synthetic sensitizers, such as ruthenium-based dyes in terms of performance (power output and efficiency), the natural dye extract proposed here are far more economical and are readily available.

MATERIALS AND METHODS

Photo-electrode and counter-electrode preparation

The photo-electrode was used as-received from Solaronix (http://shop.solaronix.com/solar-cell-kits/test-cell-kits/test-cell-spare-parts.html). It is composed of glass substrates of 20 × 20 × 2 mm with a coating of TCO22-7 FTO. The 6 × 6 mm active area of titania coating consists of an active layer of Titanium nanoxide covered by a reflective layer of Titanium nanoxide, both of which were prepared by screen-printing. The electrodes were fired up to around 400 °C for 30 minutes and left to cool to around 60 °C before being immersed in the dye solution. The counter electrode substrate, also used as-received from Solaronix, comprises of the same dimensions of the photo-electrode and FTO coating. The 20 × 20 mm active area was prepared by screen-printing for a homogenous surface using the Platisol T/SP precursor.

Dye Extraction

The leaves were first rinsed thoroughly with water and left to dry in air. 4.23 g of the leaves with an average surface area of 1 cm^2 were placed in 25 mL of ethanol and degassed for 10 minutes. The leaves were then sonicated for 20 minutes, after which the leaves were filtered out and the remaining solution was filtered through a PTFE syringe filter of 0.45 μm pores. Each electrode (now at 60 °C) was submerged in 7 mL of the solution. The dye was covered and stored in a dark environment overnight for dye adsorption.

Powder Composition

XRF (X-ray fluorescence) from Horiba, XGT 7200 operating with a Rh target, a tube voltage of 50 kV and tube current of 1mA is used to determine the elemental composition of the dye materials.

Optical Characterization

Optical characterizations were carried out via Maya 2000-Pro high-resolution spectrometers (OceanOptics). The dedicated spectrometer measured a wavelength range from 400 nm to 800 nm with a resolution of 0.2 nm. For reflectance measurement, we used a ISP-REF integrating sphere with a WS-1 reflectance standard for reflectance calibration from OceanOptics. The transmissivity of the stained titania electrodes was measured an HL-2000 tungsten halogen light source and was converted into absorbance by Eq. 1 (SHU, 2018).

$$A(a.u) = 2 - \log(\%T) \quad (1)$$

The integrating sphere (OceanOptics ISP-REF, with a sample aperture of 0.4 inch) has a built-in tungsten halogen light source (Ocean Optics LS-1-LL) and is capable of

measuring specular and diffuse reflectance. The reflectance standard is used to store baseline absorptance (0%) spectra to facilitate comparison between the various compositions.

Solar Cell Assembly

After the staining process, the photoelectrode was rinsed by ethanol to remove any excess dye residues and was allowed to dry in air. The powder from the bottom of the Calotropis leaf was carefully tapped onto the active area of the stained substrate with an amount equivalent to an area of 0.5 cm^2 on the leaf is added to the solution.

Subsequently, a Meltonix 1170-60 sealing film gasket was placed around electrode active area and the space was filled with an iodide/tri-iodide based electrolyte (Iodolyte AN-50 from Solaronix). The DSSC was then assembled by placing the photoelectrode and counterelectrode in place with binder clips.

Cell performance testing and temperature response study/impedance testing

The current-voltage (*I-V*) measurements of DSSCs were carried out with a Keithley 2400 SourceMeter under an ABET SunLite solar simulator at AM1.5G and 1,000 W m^{-2} irradiance at room temperature (25 °C).

Impedance spectra were obtained using an impedance analyzer potentiostat (VSP-300) under illumination with the sun simulator. An AC signal of 14.2 mV was applied to the cell under 1-Sun conditions. The frequency range was varied between 100 kHz and 0.1 Hz with a fixed applied bias voltage of the open circuit potential of the DSSC with a potential resolution of 20 μV. The spectra were fitted using the Z-Fit analysis software from Bio-logic.

RESULTS AND DISCUSSION

Powder composition

The XRF analysis of the powder material found covering the *Calotropis* leaves has revealed that it is composed mainly of calcium (~60%), chlorine (~16%) and iron (~8%) and the rest are traces of various elements that registered on both top and bottom leaf surfaces. The optical effect of this material manifest in terms of heat input mitigation, as a radiation scattering mechanism that is coupled with the leaf reflectivity. In this work, the powder will also be added to the extracted dye to capitalize on the ionic species that appear to exist in its composition. The full XRF analysis of the *Calotropis* leaves is shown in Table 1. Fig. 1 (a) and (b) also show the leaves with and without powder, respectively.

Table 1. Summary of XRF analysis of *Calotropis* leaves

Element	Mg	Si	P	S	Cl	K	Ca	Ti	Cr	Mn	Fe	Ni	Zn	Sr
Mass %	4.15	8.33	0.77	5.70	7.58	0.96	59.42	0.83	0.15	0.71	10.36	0.28	0.25	0.51

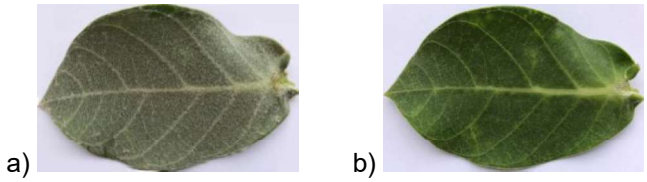

Figure 1. Calotropis leaves
a) with powder and
b) without powder.

Optical properties

The effect of the presence of the powder material on the leaves (before crushing) and on the dye extract (after crushing) is investigated. The reflectivity of the leaves is measured from both sides (top and bottom) for the as-is leaves (with powder) and for cleaned leaves (without powder). For the latter case, both sides showed similar reflectivity trends over the test spectrum (400–800 nm) with the top side exhibiting less reflective losses especially in the visible region, as shown in Fig. 2 (a).

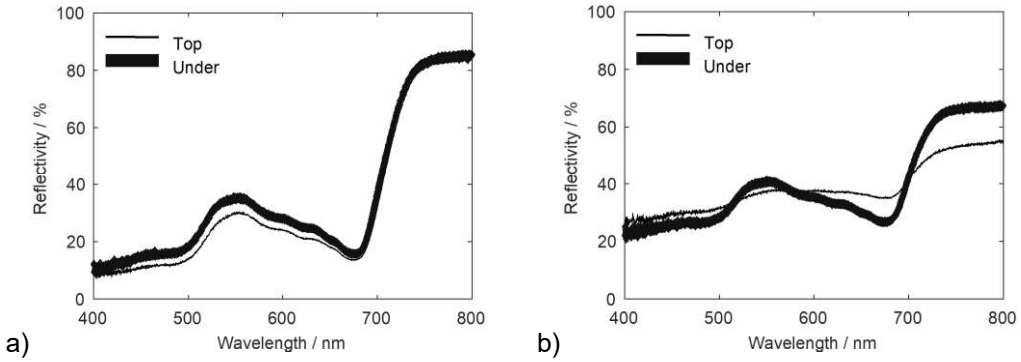

Figure 2. Reflectivity measurement for leaves (a) cleaned from powder and (b) with powder layer intact.

The as-is leaves shows a big decrease of reflectivity in close to the infrared region, with the top side exhibiting a less pronounced knee around the 680 nm mark compared with the bottom side as seen Fig. 2 (b). The reflectivity of the bottom side in the infrared region for the with-powder case is also around 44% more than the top side. These trends indicate that the enhanced reflectivity of the bottom surface of the leaves work to direct any stray rays to the top surface of adjacent leaves by reflecting off their bottom surface. This is especially true for a small portion of the visible region (between ~ 520–270 nm) and also for the NIR portion between 700–800 nm.

The powder itself as a solid-state material, however, exhibits different reflectivity depending on the side from which it has been collected as seen in Fig. 3.

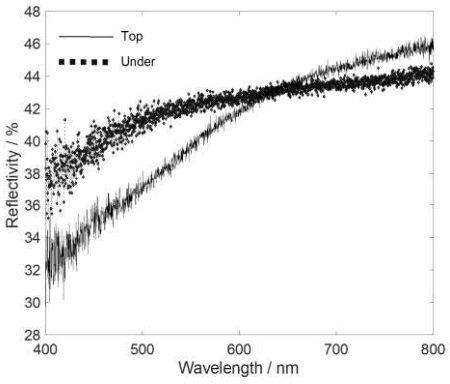

Figure 3. Reflectivity of the powder material.

The bottom powder is more reflective between 400–600 nm, while its counterpart from the top takes over after 650 nm, allowing more absorbance of the low energy incidence on the topside, mainly to mitigate heat generation within the plant.

Following the dye extraction from *Calotropis* leaves, another optical assessment was conducted by applying the dye on a photoelectrode (FTO with TiO_2 deposit). Fig. 4 shows its absorbance results compared with a bare TiO_2 reference, and another electrode soaked with the chlorophyll II pigment source (spinach), which is a common natural sensitizer used in literature (Chang et al., 2010). The bandgaps are also calculated and shown in inset.

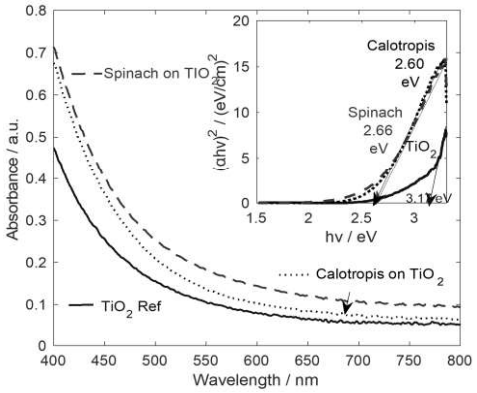

Figure 4. Spectral absorbance of *Calotropis* dye compared with a bare titania photoelectrode and another soaked in spinach (chlorophyll II). The bandgaps are calculated via T_{auc} formula.

The absorbance curves show the expected higher spectral absorbance at the violet-blue region for both spinach and the *Calotropis* dyes, with the former leveling off at the edge of the visible region as the latter continues its decline towards the infrared regime. As will be explained later, this has a noticeable effect in enhancing cell performance with less heat-generating radiation being absorbed into the photoelectrode.

Impedance test

To test for applicability of the dye to be used in DSSCs, further details into the workings of the cell are discussed with the aid of impedance spectra.

The impedance test results and its frequency response are shown in Figs 5 and 6. It is evident from Fig. 5 that the overall shape of the EIS spectra is characteristic of DSCs obtained at open circuit potential (Gamry, 2018). There is a bulge at high frequencies followed by a wide semicircle at intermediate frequencies and ending with a tail at low frequencies. This indicates that the cell construction is good for the current test conditions.

The arc observed at high frequencies (shown inset of Fig. 5), is attributed to the charge transfer processes at the counter-electrode/electrolyte interface. It is not very pronounced which indicates that the electrode is still active and could be enhanced/pre-treated for better cell performance.

At intermediate frequencies, the wide peak seen is attributed to the electron diffusion in the TiO_2 film and the electron transfer at the TiO_2/electrolyte interface. It is evident that the diameter of the semicircle in the intermediate frequency region was large proving the capability of the effective suppression of the back reaction of the injected electrons with tri-iodide species in the electrolyte, this leads to a relatively high value of photovoltage.

At low frequencies, the tail of the peak corresponds to a slow diffusion process of I_3^- in the electrolyte. With time and at relatively high illumination, the electrolyte loses its viscosity making it harder to transport ions through the electrolyte and this peak would disappear. This peak usually becomes more pronounced for fully degraded cells because of the increase in tri-iodide species in the electrolyte that is seen to accelerate the recapture of electrons in the conduction band, which in turn reduces availability within the oxide layer. For the case at hand, the concentration of the tri-iodide species is of a relatively low concentration compared to iodide species and is seen as an advantage to reduce charge recombination and its adverse effect on cell performance.

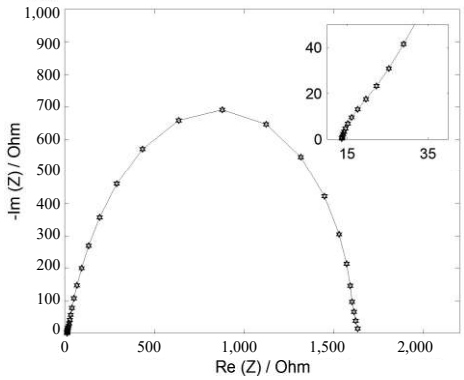

Figure 5. Nyquist plot of tested cell.

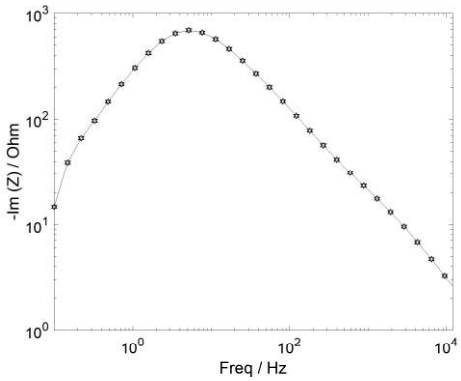

Figure 6. Frequency response of the tested cell.

The Bode plot of the assembled cell is shown in Fig. 6 for the frequency response of the cell. The more the main peak shifts to the right, the higher the rate of transfer at TiO_2/dye/electrolyte interface. It can be observed that the cell is not performing at optimal conditions, which means that better efficiencies can be obtained from the cell with more appropriate ambient test conditions (e.g. irradiance, temperature, electrolyte concentration).

Cell testing

DSSCs using dyes extracted from the leaves of *Calotropis* (with and without the powder on the leaves of *Calotropis* added onto the stained photoelectrode) were assembled and tested at room temperature under simulated 1-sun AM1.5G irradiance. As a reference, a DSSC using dye extracted from spinach was also tested, which is a proven robust natural dye in DSSC studies (Syafinar et alю, 2015). The current density-voltage (J-V) characteristic curves are plotted in Fig. 7 along with the experimental error bars, while the corresponding photovoltaic parameters of these DSSCs are summarized in Table 2.

From the results, both solar cells using dye extracted from *Calotropis* (with and without adding powder) showed better performance compared to the spinach cell, suggesting that the dye from *Calotropis* can be served as an excellent natural light sensitizer. Furthermore, it is evident that the addition of the powder from the *Calotropis* leaves led to an overall performance enhancement in *Calotropis*-based DSSCs. Notably, the open circuit voltage (V_{OC}) was improved from 0.410 to 0.573 V and fill factor (FF) was increased from 47.6% to 63.2%. This considerable improvement in FF is due to the

addition of the powder material and the more efficient charge transfer process it introduces between the dye and the redox couple, as indicated in literature (Al-Alwani et al., 2015). These findings are also consistent with our findings from the impedance tests described above. In addition, the short-circuit current density (J_{SC}) increased slightly from 0.555 to 0.592 mA cm^{-2} which may correspond to the changes in cell optical reflectivity as measured in Fig. 3. Consequently, the power conversion efficiency (PCE) of DSSCs using *Calotropis* dye was significantly enhanced from 0.108% to 0.214%.

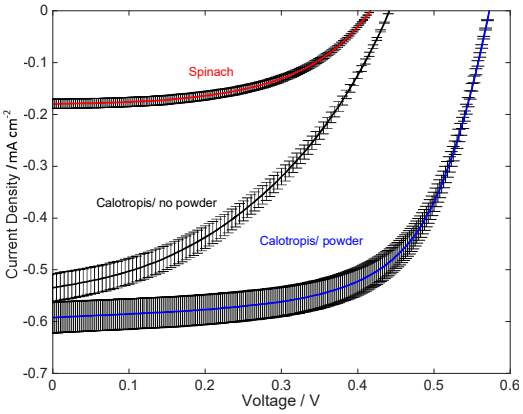

Figure 7. Current density-voltage (*J-V*) characteristics of DSSCs using dyes from *Calotropis* and spinach, shown with experimental error bars.

Table 2. Summary of photovoltaic parameters for DSSCs

Parameter	Spinach	Calotropis (no powder)	Calotropis (with powder)
J_{sc}, mA cm^{-2}	0.18	0.55	0.59
V_{oc}, V	0.41	0.41	0.57
FF, %	52.70	47.60	63.20
PCE, %	0.04	0.11	0.21

CONCLUSIONS

This work assessed the performance enhancement of solar cells sensitized via a natural dye extracted from a non-food plant (*Calotropis*) that is both native to and abundant in the desert regions of the United Arab Emirates. The dye used in a number of dye-sensitized solar cells has shown good enhancement of power output and efficiency (~67% more power and ~87% more power) compared with a common natural sensitizer (spinach). The *Calotropis* leaves are also covered with a powder that is thought to help mitigate heat generated within the leaf due to incident radiation in the harsh desert climate. This presence of this powder on the leaf prompted using it with the extracted dye (leaves are used without cleaning off the powder), as its composition shows a significant number of ionic species that would enhance the catalytic activity of the cell. This is proven when another set of cells were constructed with powder added to *Calotropis* dye extracts showed a further significant enhancement on the power, fill factor and efficiency. The latter reached 0.214%, a 50% enhancement over its non-powder counterpart. The future work will include better dye.

REFERENCES

Al-Alwani, M.A.M, Mohamad, A.B, Kadhum, A.A.H. & Ludin, N.A. 2015. Effect of solvents on the extraction of natural pigments and absorption onto TiO2 for dye-sensitized solar cell applications. Spectrochimica Acta Part A: *Molecular and Biomolecular Spectroscopy* **138**, 130–137.

Bhattacharya, S. Chakrabarti, H. & Reehal, V. Lakshminarayanan (eds). *Advances in optical science and engineering*. Springer proceedings in physics, vol. **194**. Springer, Singapore.

Bloomberg new energy finance. New energy outlook 2015. BNEF: London, 2015; June 23.

Breyer, C., Bogdanov, D., Gulagi, A., Aghahosseini, A., Barbosa, L.S.N.S., Koskinen, O., Barasa, M., Caldera, U. Afanasyeva, S., Child, M., Farfan, J. & Vainikka, P. 2017. On the role of solar photovoltaics in global energy transition scenarios. Prog. Photovolt: *Res. Appl*. **25**, 727–745.

Chang, H. & Lo, Y. 2010. Pomegranate leaves and mulberry fruit as natural sensitizers for dye-sensitized solar cells. *Solar Energy* **84**(10), 1833–1837.

Chang, H., Wu, H., Chen, T., Huang, K., Jwo, C. & Lo, Y. 2010. Dye-sensitized solar cell using natural dyes extracted from spinach and ipomoea. *Journal of Alloys and Compounds* **495**(2), 606–610.

Choubey, P.C., Oudhia, A. & Dewangan, R. 2012. *A review: solar cell current scenario and future trends*. Recent Research in Science and Technology 4. pp. 99–101.

Gamry.com. 2018. *Dye Solar Cells - DSC - Impedance Measurements, application note*. [online] Available at: https://www.gamry.com/application-notes/physechem/dye-solar-cells-impedance-measurements/ [Accessed 9 Feb. 2018].

Ghosh, K. 2017. Status and Technology of Present Day Solar Cells. *Springer Proceedings in Physics*, pp.19–28.

Hosenuzzaman, M., Rahim, N.A., Selvaraj, J., Hasanuzzaman, M., Malek, A.B.M.A. & Nahar, A. 2015. Global prospects, progress, policies, and environmental impact of solar photovoltaic power generation. *Renewable and Sustainable Energy Reviews* **41**, 284–297.

Jones, H.G. & Rotenberg, E. 2011. *Energy, Radiation and Temperature Regulation in Plants*. In: eLS. John Wiley & Sons, Ltd: Chichester.

Kaltiya, J.M.S., Abubakar, M.S. & Itodo, I.N. 2014. Prediction of global solar radiation using Angstrom-Page equation model for Makurdi Benue State, Nigeria. *American Journal of Engineering Research* **3**, 145–150.

Liu, Y., You, S., Tan, J., Zhang, Y. & Liu, Y. 2018. Frequency response assessment and enhancement of the U.S. power grids towards extra-high photovoltaic generation penetrations – an industry perspective. *IEEE Transactions on Power Systems* **PP**(99), 1–1.

Makrides, G., Zinsser, B., Norton, M., Georghiou, G.E., Schubert, M. & Werner, J.H. 2010. Potential of photovoltaic systems in countries with high solar irradiation. *Renewable and Sustainable Energy Reviews* **14**(2010), 754–762.

O'Regan, B. & Gratzel, M. 1991. A low-cost, high-efficiency solar cell based on dye-sensitized colloidal TiO2 films. *Nature* **353**, 737–740.

Phinikarides, A., Makrides, G., Zinsser, B., Schubert, M. & Georghiou, G.E. 2015. Analysis of photovoltaic system performance time series: Seasonality and performance loss. *Renew. Energy* **77**, 51–63.

Polman, A., Knight, M., Garnett, E.C., Ehrler, B. & Sinke, W.C.2016. Photovoltaic materials: Present efficiencies and future challenges. *Science* **352**, 307–315.

Raghwa, G. 2014. *Life in the plant kingdom*. Developed Environment Agency – Abu Dhabi (EAD) and the Energy and Resources Institute (TERI), United Arab Emirates, ISBN 978-9948-20-720-7.

Rahimi, M. 2015. Pharmacognostical Aspects and Pharmacological activities of Calotropis procera. *Bull. Env. Pharmacol. Life Sci.* **4**. pp. 156–162.

Renewable energy policy network for the 21st century. Renewables 2016 – global status report, Paris. 2016. www.ren21.net/wp-content/uploads/ 2016/06/GSR_2016_Full_Report_REN21.pdf.

Ritchie, R. 2006. Consistant sets of spectrophotometric chlorophyll equations for acetone, methanol and ethanol solvents. *Photosyn Res*. **89**(1), 27–41.

Said, Z., Alshehhi, Abdulla, A. & Mehmood, A. 2018. Predictions of UAE's renewable energy mix in 2030. *Renewable Energy* **118**, 779–789.

Sharma, S., Jain, K.K. & Sharma, A. 2015. Solar cells: In research and applications—a review. *Materials Sciences and Applications* **6**, pp 1145–1155.

Sharma, S., Siwach, B., Ghoshal, S.K. & Mohan, D. 2017. Dye sensitized solar cells: From genesis to recent drifts. *Renewable and Sustainable Energy Reviews* **70**, 529–537.

Sheffield Hallam University. 2018. *Beer's Law*. Sheffield: Sheffield Hallam University.

Sherwani, A.F., Usmani, J.A. & Varun. 2010. Life cycle assessment of solar PV based electricity generation systems: A review. *Renewable and Sustainable Energy Reviews* **14**, 540–544.

Shockley, W. & Queisser, H.J. 1961. Detailed balance limit of efficiency of p-n junction solar cells. *Journal of Applied Physics* **32**, 510–519.

Smith, Y. & Bogust, P. 2018. Review of Solar Silicon Recycling. *Energy Technology* **2018**, 463–470.

Syafinar, R., Gomesh, N., Irwanto, M., Fareq, M. & Irwan, Y. 2015. Chlorophyll Pigments as Nature Based Dye for Dye-Sensitized Solar Cell (DSSC). *Energy Procedia* **79**, 896–902.

Wang, H., Munoz-Garcia, M.A., Moreda, G.P. & Alonso-Garcia, M.C. 2017. Seasonal performance comparison of three grid connected photovoltaic systems based on different technologies operating under the same conditions. *Solar Energy* **144**, 798–807.

Wu, J., Lan, Z., Lin, J., Huang, M., Huang, Y., Fan, L. & Luo, G.2015. Electrolytes in Dye-Sensitized Solar Cells. *Chemical Reviews* **115**, 2136–2173.